Cell Reports
Article

Cell-Cycle Kinases Coordinate the Resolution of Recombination Intermediates with Chromosome Segregation

Joao Matos,[1] Miguel G. Blanco,[1] and Stephen C. West[1,*]
[1]London Research Institute, Cancer Research UK, Clare Hall Laboratories, South Mimms, Herts EN6 3LD, UK
*Correspondence: stephen.west@cancer.org.uk
http://dx.doi.org/10.1016/j.celrep.2013.05.039

SUMMARY

Homologous recombination leads to the formation of DNA joint molecules (JMs) that must be resolved to allow chromosome segregation, but how resolution is temporally coupled with chromosome segregation is unknown. Here, we have analyzed the role of the cell-cycle kinases Cdk and Cdc5 in coordinating these events through their involvement in the phosphoregulation of the Mus81-Mms4 nuclease. By identifying *CDC5* and *MMS4* mutants that uncouple Mus81-Mms4 activation from cell-cycle progression, we show that JM disengagement, prior to anaphase initiation, safeguards chromosome segregation. By simultaneously stimulating the cleavage of cohesin and activating Mus81-Mms4 at the G2/M transition, Cdk and Cdc5 coordinate the sequential elimination of all chromosomal interactions in preparation for chromosome segregation. Conversely, untimely Cdc5 expression increases crossover frequency due to premature activation of Mus81-Mms4. Therefore, temporal restriction of JM resolution, imposed by Cdk/Cdc5, minimizes the potential for loss of heterozygosity while preventing chromosome missegregation and aneuploidy.

INTRODUCTION

The establishment of physical interactions between chromosomes underpins vital cellular processes such as chromosome segregation and DNA repair. The timely severance of all such chromosomal connections, however, is necessary to ensure sister chromatid separation at anaphase, as failure in chromatid disjunction compromises the stable inheritance of the replicated genome and generates aneuploidy.

Sister chromatid cohesion (SCC) is required for the segregation of sister chromatids to opposite poles at anaphase. SCC disengagement is regulated by polo-like kinases that stimulate cohesin cleavage and chromosome segregation (Alexandru et al., 2001). However, problems with replication fork progression, or DNA damage, can lead to recombination between sister chromatids (and sometimes homologous chromosomes), leading to the formation of DNA joint molecules (JMs) (Bzymek et al., 2010). While these interactions are essential for DNA repair, it is critically important that JMs are processed prior to chromosome segregation. Precisely how these two events are coordinated within the cell is unknown.

In addition to eliminating chromosome connections, JM processing is equally important for determining the outcome of recombination. For example, during meiosis, crossover (CO) recombinants are required for the segregation of homologous chromosomes, whereas in mitotic cells noncrossover (NCO) formation is favored in order to avoid sister chromatid exchanges (SCEs) and the potential for loss of heterozygosity (LOH). To prevent CO formation, mitotic cells disengage JMs at an early stage by the use of antirecombinogenic helicases (Ira et al., 2003). Alternatively, JMs that are covalently linked by four-way DNA junctions, also known as Holliday junctions (HJs), can be "dissolved" by the Sgs1-Top3-Rmi1 (STR) complex in yeast, or BLM-TOPIIIα-RMI1-RMI2 (BTR) in humans, to generate NCOs (Wu and Hickson, 2003).

In addition to junction dissolution and NCO formation, mitotic JMs can be "resolved" to form COs by nucleases such as Mus81-Mms4 (human MUS81-EME1) and Yen1 (human GEN1) (Ip et al., 2008; Kaliraman et al., 2001). Mus81-Mms4 plays an important role in DNA repair and serves as a backup for Sgs1-Top3-Rmi1 in JM processing (Ashton et al., 2011; Dayani et al., 2011). Similarly, Yen1 provides an additional backup to Mus81-Mms4 (Blanco et al., 2010; Ho et al., 2010; Tay and Wu, 2010).

The presence of multiple pathways for JM processing highlights the importance placed on ensuring that recombination intermediates will not constitute a physical barrier to chromosome segregation. However, because the outcome (NCO versus CO) of JM processing differs according to the pathway used (dissolution versus resolution), the formation of COs needs to be tightly regulated. Recent studies indicate that this is achieved by coupling the activities of Mus81-Mms4 and Yen1 to cell-cycle progression (Gallo-Fernández et al., 2012; Matos et al., 2011; Szakal and Branzei, 2013). During meiosis, Cdk- and Cdc5-mediated phosphorylation of Mms4 hyperactivates Mus81-Mms4 in late pachytene, thereby ensuring that JMs are processed in time for meiosis I. Conversely, Yen1 is held in check

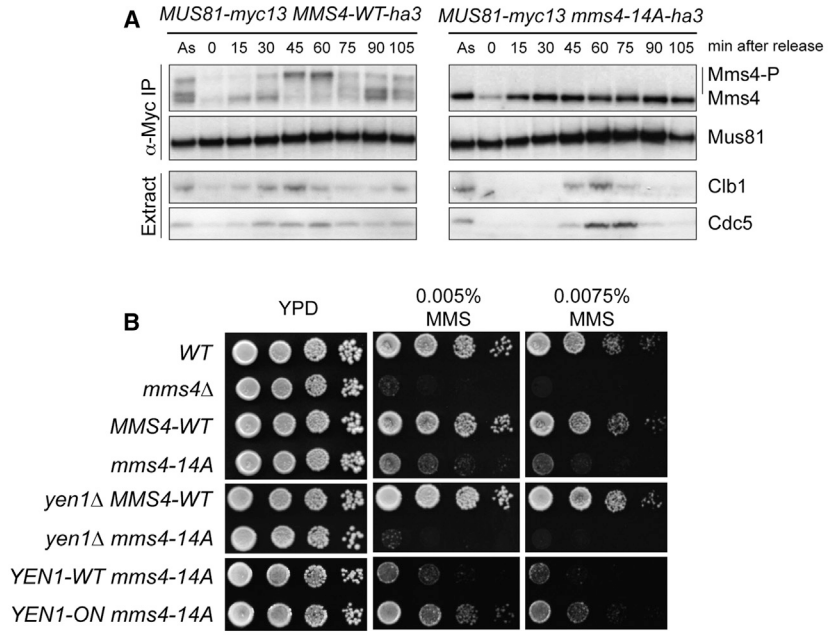

Figure 1. Mms4 Phosphorylation Depends on Cdk and Cdc5 and Is Required for Efficient DNA Repair

(A) Mitotic time courses comparing the phosphorylation of Mms4 and Mms4-14A. Cells were synchronized using α-factor and samples taken at various times after release. Following affinity purification of Mus81-myc13, the immunoprecipitates were western blotted for the indicated proteins.

(B) DNA damage sensitivity assays were carried out by analyzing 10-fold serial dilutions of cells grown to mid-log phase, normalized, and then spotted onto YPD plates containing the indicated amounts of MMS. Cells were grown for 2 days at 30°C.

(C–E) Protein extracts were prepared from nocodazole-treated cells expressing *MMS4-myc9*. Mms4-myc9 and Clb1 were detected by western blotting, and Mms4-myc9 was affinity purified from each extract and assayed for Mms4 phosphorylation and Mus81-Mms4 mediated HJ resolution activity. (C) *CDC28 or cdc28-as1* cells were collected after treatment with the Cdc28-as1 kinase inhibitor 1NM-PP1. (D and E) *CDC5* or *cdc5-2* cells were collected after 1 hr incubation at 37°C or 25°C, as indicated. See also Figure S1.

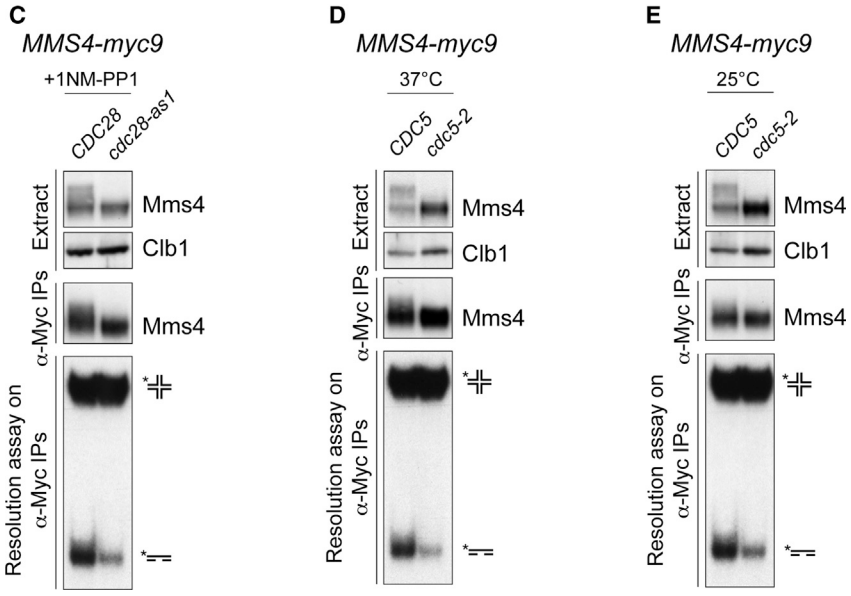

by inhibitory phosphorylation until the onset of meiosis II. Related posttranslational modifications regulate Mus81-Mms4 and Yen1 activities in mitotic cells such that they are activated at the G2/M transition and anaphase, respectively.

Here, we have analyzed the roles of the cell-cycle kinases Cdk and Cdc5 in coordinating the disengagement of mitotic recombination intermediates with chromosome segregation. We find that Cdk/Cdc5-mediated activation of Mus81-Mms4, at the G2/M transition, ensures the timely initiation of anaphase and prevents chromosome missegregation. By stimulating separase-mediated cohesin cleavage and activating Mus81-Mms4, Cdk and Cdc5 coordinate the sequential elimination of both protein- and DNA-based chromosomal interactions. Temporal control of Mus81-Mms4 activity depended on the cell-cycle-regulated expression of Cdc5. Consistent with this notion, uncontrolled Cdc5 expression caused the premature activation of Mus81-Mms4, altering the CO/NCO ratio and increasing the potential for loss of heterozygosity.

RESULTS

JM Resolution Prior to Anaphase Initiation Is Required for Efficient DNA Repair

Mus81-Mms4 becomes hyperactivated at the G2/M transition, and activation correlates with the phosphorylation of Mms4 and the accumulation of cyclin-dependent kinase and the polo-like kinase Cdc5 (Gallo-Fernández et al., 2012; Matos et al., 2011). To analyze the role of Mms4 phosphorylation in DNA repair, we generated *mms4-14A*, which has 14 of the identified/predicted G2/M phosphorylation sites mutated to alanine (Figure S1) (Matos et al., 2011). Mms4-14A protein associated normally with Mus81 but exhibited reduced phosphorylation compared to Mms4 upon accumulation of Cdc5 and the mitotic cyclin Clb1 (Figure 1A). As a consequence, *mms4-14A* strains showed significant sensitivity to DNA damaging agents such as methyl methanesulfonate (MMS), although the repair deficiency was not as great as that seen with *mms4Δ* cells (Figure 1B). Repair deficiency was increased 100-fold by deletion of *YEN1*, consistent with Yen1 acting as a backup to phosphoactivated Mus81-Mms4.

Despite providing a backup for Mus81-Mms4, Yen1 could not fully suppress the DNA repair defects of *mms4-14A* mutants, implying that the functional overlap between both nucleases is only partial. Since Mus81-Mms4 phosphorylation occurs at the G2/M transition, whereas Yen1 is activated later, at anaphase, we determined whether differences in the timing of activation might explain the inability of Yen1 to fully compensate for the lack of Mus81-Mms4 function. To do this, we generated a Yen1 mutant (*YEN1-ON*) that is resistant to inhibitory phosphorylation and is constitutively active throughout the cell cycle (M.G.B., J.M., and S.C.W, unpublished data) to find out whether premature activation of Yen1 could suppress the DNA repair defects of *mms4-14A* cells. Complementation of *yen1Δ mms4-14A* double mutants with *YEN1-ON* led to a significant increase in MMS resistance relative to *YEN1-WT* (Figure 1B).

These results show that G2/M phosphorylation of Mms4 is required for an essential subset of the DNA repair functions of Mus81-Mms4. Moreover, the functional overlap with Yen1 indicates that activated Mus81-Mms4 is important for JM processing and that JM processing prior to anaphase initiation is crucial for an efficient DNA damage response.

Cdk and Cdc5 Hyperactivate Mus81-Mms4

To determine the roles of Cdc28/Cdk and Cdc5 in Mus81-Mms4 activation at the G2/M transition, Mms4 phosphorylation and Mus81-Mms4 nuclease activity were analyzed in immunoprecipitates of extracts prepared from cells carrying mutant alleles of the two kinases. Because *CDC28* and *CDC5* are essential for cell-cycle progression and cell viability, we used an ATP-analog-sensitive version of Cdc28 (*cdc28-as1*) and a temperature-sensitive allele of *CDC5* (*cdc5-2*, also known as *msd2-1*) (Bishop et al., 2000; Kitada et al., 1993). When *cdc28-as1* cells were synchronized at G2/M using nocodazole, the stage at which Mus81-Mms4 is normally fully phosphorylated and hyperactive (Matos et al., 2011), and treated for 30 min with the ATP-analog 1NM-PP1, we found that Mms4 phosphorylation and Mus81-Mms4-mediated HJ resolution were both severely impaired (Figure 1C). Analysis of Clb1, an M phase marker, showed that Cdc28 inhibition did not cause a dramatic change in the fraction of cells blocked at G2/M.

In similar experiments, *cdc5-2* mutants were synchronized with nocodazole at 25°C (a permissive temperature for proliferation) (Shirayama et al., 1998). Cultures were then split and incubated for 1 additional hour at either 25°C or at the restrictive temperature of 37°C. These mutants were unable to phosphorylate and activate Mus81-Mms4 after shifting up to 37°C (Figure 1D). Indeed, even at 25°C, the *cdc5-2* mutants showed a complete failure in the phosphorylation and activation of Mus81-Mms4 (Figure 1E). These results confirm that Cdk and Cdc5 collaborate to phosphoactivate Mus81-Mms4 at the onset of mitosis. Furthermore, since inhibition of either kinase in nocodazole-treated cells was sufficient to interfere with Mus81-Mms4 phosphorylation and activity, it is likely that both kinases regulate Mus81-Mms4 directly rather than through their involvement in promoting cell-cycle progression. Intriguingly, our results also suggest that, at 25°C, Cdc5-2 supports proliferation but is unable to phosphorylate or activate Mus81-Mms4.

cdc5-2: Uncoupling Mus81-Mms4 Activation from Cell-Cycle Progression

To confirm that *cdc5-2* mutants uncouple Mus81-Mms4 regulation from cell-cycle progression, the kinetics of Mms4 phosphorylation and Mus81-Mms4 activity were examined through a complete cell cycle. *CDC5* or *cdc5-2* strains expressing Mms4-myc9 were synchronized in G1 and released to undergo one round of mitosis, with samples collected at 15 min intervals. In control *CDC5* cells, Mms4 phosphorylation was observed ~75 min after release, which coincided with the accumulation of Clb1-Cdk and Cdc5 and hyperactivation of Mus81-Mms4 nuclease (Figure 2A, left). In contrast, in the *cdc5-2* mutants, even at the permissive temperature (25°C), there was a complete failure to phosphorylate Mms4 and activate Mus81-Mms4 at the G2/M transition (Figure 2A, right). Importantly, fluorescence-activated cell sorting (FACS) analysis of DNA content (Figure S2A) and western blot analysis of Clb1 (Figure 2A) showed that *cdc5-2* mutants completed DNA replication and underwent mitosis, though with slightly delayed kinetics. At the nonpermissive temperature (37°C), *cdc5-2* mutants did not phosphorylate or activate Mus81-Mms4 and proliferation failure resulted in the accumulation of cells with a G2 DNA content (Figure S2A) as well as high levels of the M phase marker Clb1 (Figure 2A, center).

Cdc5 Is Required for Efficient DNA Repair

Our studies with Cdc5-2 showed that the kinase fails to promote Mms4 phosphorylation under permissive conditions and yet supports all the essential functions of Cdc5 required for cell-cycle progression and chromosome segregation. This ability to uncouple Mms4 phosphorylation from cell-cycle progression provided a unique and powerful tool to examine the role of Cdc5 in DNA repair. The nature of the Cdc5-2 mutation was determined, revealing three mutations (D308N, E309K, and G310N) within the serine/threonine kinase domain (Figure S2B). Structural modeling indicated that acidic residues D308 and E309 are likely to be surface contact residues (Figure S2C), indicating that their substitution with neutral and basic residues (N and K) might change the ability of the Cdc5-2 kinase to efficiently modify a subset of substrates. One such substrate appears to be Mms4, leading us to predict that *cdc5-2* strains would be sensitive to DNA lesions that require Mus81-Mms4 phosphoactivation for repair.

This hypothesis was tested by growing *cdc5-2* strains at 25°C followed by exposure to a variety of DNA damaging agents. The *cdc5-2* strains showed an exquisite sensitivity to DNA damage and were up to 1,000-fold more sensitive than the corresponding wild-type strains to MMS (Figure 2B; Figure S2D). Indeed, the damage sensitivity of *cdc5-2* was comparable to that seen with *mms4Δ* mutants, and with *mms4Δ cdc5-2* double mutants. Similar results were observed with agents such as hydroxyurea, camptothecin (CPT), UV light, and 4-nitoquinoline 1-oxide (4-NQO).

These results indicate that Cdc5, a central regulator of cell-cycle and chromosome segregation, also acts as a direct regulator of DNA repair. Cdc5 and Mus81-Mms4 appear to operate in the same DNA repair pathway, consistent with Cdc5-mediated phosphorylation of Mms4 being the key molecular function of Cdc5 in promoting the processing of DNA repair intermediates.

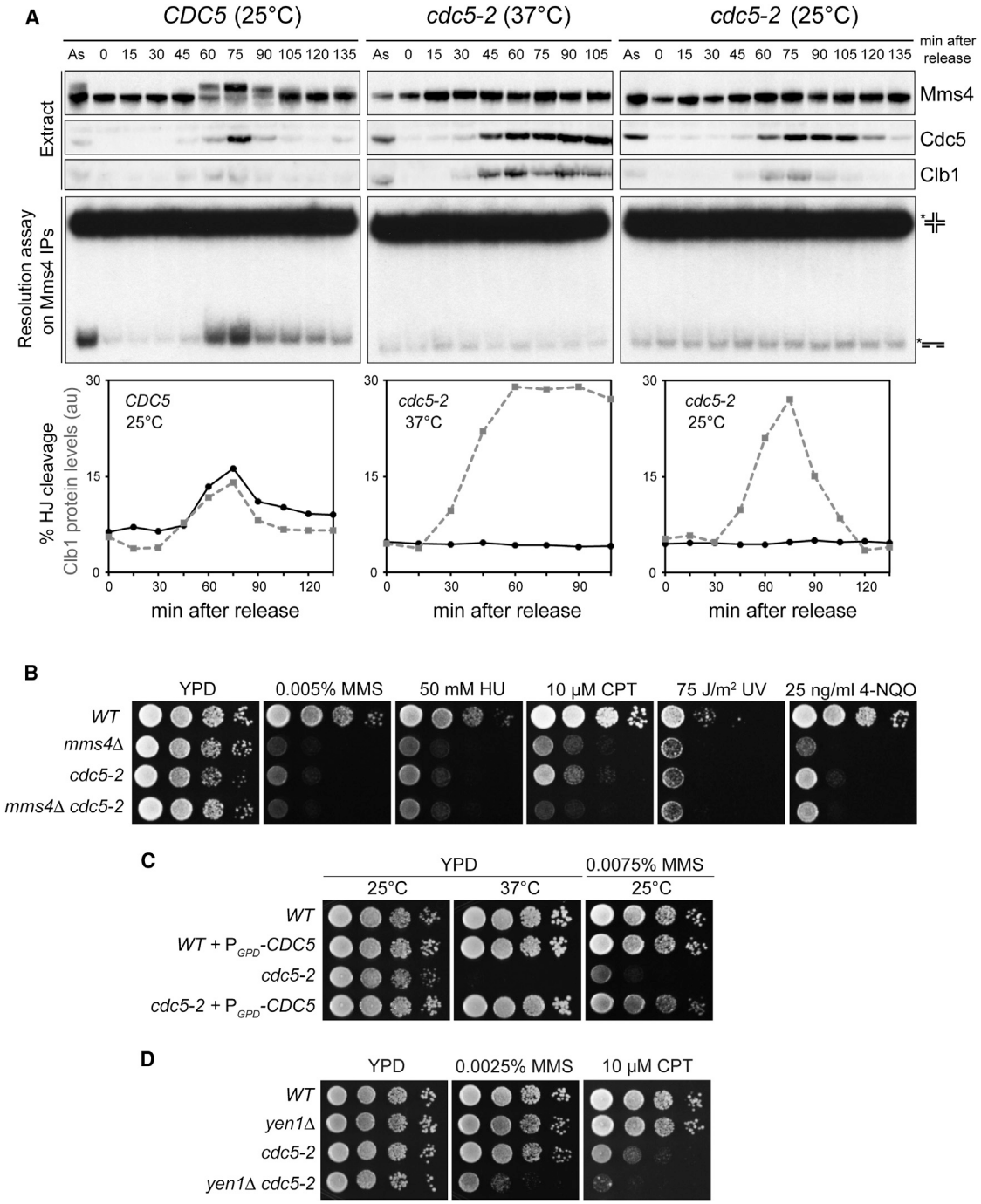

Figure 2. Cdc5 Is Required for Efficient DNA Repair

(A) *CDC5* or *cdc5-2* strains expressing *MMS4-myc9* were synchronized by α-factor treatment and released at the indicated temperatures. Extracts were prepared and affinity-purified Mms4 was assayed for HJ resolution activity. Graphical display of the quantification of HJ resolvase activity relative to the kinetics of Clb1 accumulation is shown. As, sample taken from asynchronous proliferating cells.

(B) DNA damage sensitivity of *cdc5-2* mutants, analyzed as described for Figure 1B. Cells were grown for 3 days at 25°C.

(C) Complementation of *cdc5-2* mutant strains with P_{GPD}-*CDC5*. As in (B), except the cells were grown at the indicated temperatures.

(D) Deletion of *YEN1* increases the DNA damage sensitivity of *cdc5-2* mutants.

See also Figure S2.

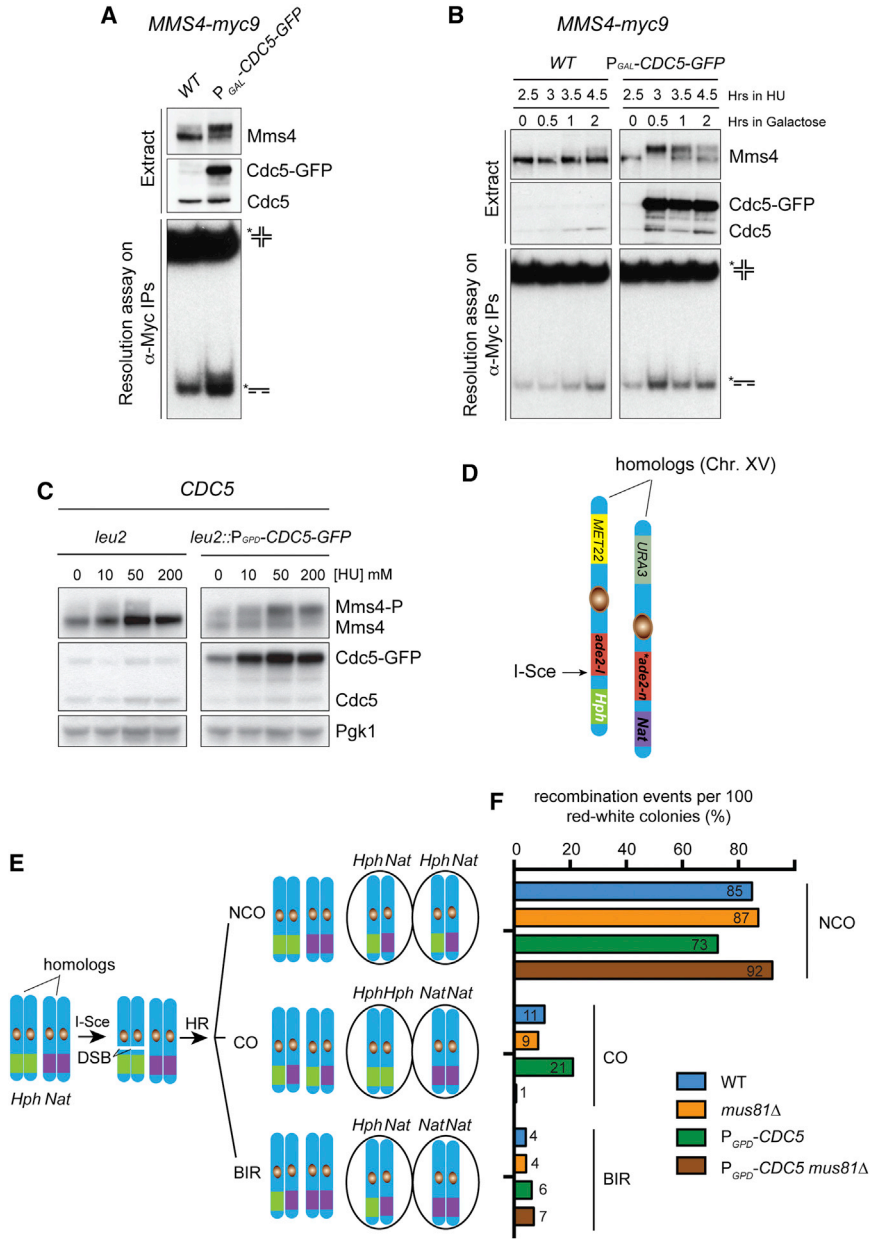

Figure 3. Unregulated Cdc5 Expression Causes Premature Mus81-Mms4 Activation and Increases CO Frequency

(A) Wild-type or cells expressing Cdc5-GFP from the inducible *GAL1* promoter were treated with galactose for 2 hr. Extracts were prepared and analyzed for the presence of the indicated proteins by western blotting. Mms4-myc9 was affinity-purified and assayed for HJ resolution activity.

(B) The cells used in (A) were treated with hydroxyurea for 2.5 hr and Cdc5 was induced by the addition of galactose. Samples were collected at the indicated time points and analyzed as in (A).

(C) Wild-type or cells expressing Cdc5-GFP from the *GPD1* promoter were treated with increasing concentrations of HU for 3 hr. Extracts were prepared and analyzed by western blotting.

(D) Schematic representation of chromosome XV homologs in the diploid strains used in (F), showing the I-SceI cut site and the *ade2-n* mutation (*).

(E) Representation of interhomolog recombination events resulting from the repair of I-SceI-mediated DSBs in both sisters, using a non-sister chromatid as template. NCO, noncrossover; CO, crossover; BIR, break-induced replication.

(F) Distribution of NCO, CO, and BIR products for red-white (*ade2/ADE2*) sectored recombinant colonies of the indicated genotypes.

See also Table S1.

As expected, *CDC5-WT* complemented *cdc5-2* strains, confirming that the observed defects are directly attributable to the integrity of Cdc5 and are not a consequence of any gain of function conferred by the Cdc5-2 protein (Figure 2C). Deletion of *YEN1* from *cdc5-2* strains led to an increased sensitivity to MMS and CPT-induced DNA damage (Figure 2D; Figure S2E), consistent with it providing a backup pathway for phosphoactivated Mus81-Mms4.

Premature Activation of Mus81-Mms4 Increases Crossover Frequency

To determine whether Cdc5 expression was sufficient for Mus81-Mms4 phosphorylation and activation, we analyzed strains carrying *CDC5-GFP* under the control of the galactose-inducible promoter (P_{GAL}-*CDC5*). Addition of galactose to the media triggered the robust accumulation of Cdc5-GFP (Figure 3A), an increase in the fraction of phosphorylated Mms4, and, importantly, the hyperactivation of Mus81-Mms4 nuclease. FACS analysis of DNA content revealed a modest increase in the population of cells with a G2 DNA content in response to Cdc5 overexpression (data not shown).

To ensure that the Mus81-Mms4 activation was not an indirect consequence of a cell-cycle delay, we tested the effect of Cdc5 overexpression in cells synchronized at G1/S using the ribonucleotide reductase inhibitor hydroxyurea (HU). After HU treatment (t = 2.5 hr), control and P_{GAL}-*CDC5* cells accumulated with a G1 DNA content, nonphosphorylated Mms4, and low levels of Mus81-Mms4 activity (Figure 3B and data not shown), as expected. However, 30 min after galactose addition, Cdc5-GFP expression triggered the rapid phosphorylation of Mms4 and hyperactivation of Mus81-Mms4. These results show that Cdc5 is directly responsible for the phosphorylation-dependent activation of Mus81-Mms4.

The ability to prematurely activate Mus81-Mms4 by misregulating Cdc5 expression offered an opportunity to determine whether premature activation might allow Mus81-Mms4 to

compete with STR (Sgs1-Top3-Rmi1)-mediated HJ dissolution and thereby affect the frequency of mitotic CO formation. However, because galactose-induced Cdc5 overexpression is toxic (data not shown), we expressed Cdc5 from the constitutively active *GPD* promoter (P_{GPD}-*CDC5*), which exhibits normal rates of proliferation and resistance to MMS (Figures 2C and 3C). Importantly, cycling P_{GPD}-*CDC5* cells showed a higher proportion of phosphorylated Mms4, which was even greater when increasing amounts of HU were used to synchronize cells at G1/S, a stage at which Mms4 is normally nonphosphorylated.

To determine whether uncontrolled Cdc5 expression alters the outcome of homologous recombination, we used a well-established genetic assay that distinguishes between CO and NCO products of recombination upon site-specific induction of a double-strand break (DSB) at the *ade2* locus in diploid cells (Ho et al., 2010) (Figures 3D and 3E). We observed a marked increase in CO formation concurrent with Cdc5 overexpression, which was accompanied by a proportional decrease in NCO events (Figure 3F; Table S1). Interestingly, deletion of *MUS81* from the P_{GPD}-*CDC5* cells not only eliminated the increase in COs caused by Cdc5 overexpression but also reduced CO events to levels significantly lower than those of *mus81Δ* single mutants (Figure 3F). These results reveal that the ability to restrain Mus81-Mms4 activity to late stages of the cell cycle is critical for the control of mitotic CO formation. Furthermore, our data imply that misexpression of Mus81-Mms4 regulators, such as Cdc5, will impair the ability of mitotically proliferating cells to limit SCE formation and LOH.

Activation of Mus81-Mms4 Is Required for JM Processing and Mitotic Proliferation in the Absence of *SGS1*

The synthetic lethality of *sgs1Δ mms4Δ* double mutants is thought to result from endogenous replication stress that generates toxic recombination intermediates whose disengagement by STR or Mus81-Mms41 is essential for cell survival (Fabre et al., 2002; Mullen et al., 2001). We therefore tested whether phosphoactivation of Mus81-Mms4 was necessary to provide a backup mechanism for STR-mediated JM processing. To do this, haploid cells carrying *mms4Δ*, *MMS4-WT*, or *mms4-14A* alleles were crossed with *sgs1Δ* mutants. Microdissection of the sporulated heterozygous diploids showed the formation of microcolonies when *mms4-14A* and *sgs1Δ* cosegregated (Figure 4A). Consistent with the notion that Cdc5-mediated activation of Mus81-Mms4 is important for proliferation in *sgs1Δ* mutants, *cdc5-2 sgs1Δ* double mutants also formed microcolonies whereas *cdc5-2 mms4Δ* or *cdc5-2 mms4-14A* double mutants did not (Figure 4B).

Microscopic inspection of *sgs1Δ mms4-14A* and *sgs1Δ cdc5-2* strains revealed that both double mutants accumulated very large cells containing large buds (Figures 4C and 4D). Such a morphology is characteristic of a delayed G2/M transition or a prolonged mitosis, indicating that their slow proliferation is caused by defects in cell-cycle progression. This was confirmed by FACS analysis, which revealed an increase in cells with a G2 DNA content (Figure 4E). Expression of constitutively active Yen1-ON largely suppressed the G2/M accumulation and proliferation defects (Figures 4C–4E). We also observed the appearance, at a low frequency, of multibudded cells in *sgs1Δ mms4-14A* and *sgs1Δ cdc5-2* double mutants (Figure 4D, right panel), again consistent with the FACS detection of a population of cells containing a DNA content greater than 2N.

These data show that Cdc5-mediated phosphoactivation of Mus81-Mms4 at G2/M is required for the processing of DNA repair intermediates that accumulate in the absence of STR. Furthermore, our results indicate that, due to the late activation of Mus81-Mms4, STR provides the primary JM processing activity during DNA replication. The presence of DNA damage leads to checkpoint activation, which indirectly delays Mus81-Mms4 activation through the inhibition of Cdk and Cdc5 (Szakal and Branzei, 2013). Only when cell-cycle progression is restored upon damage removal does Mus81-Mms4 become activated for JM processing.

Joint Molecule Accumulation Delays Initiation of Anaphase

While it is known that DNA lesions trigger activation of the DNA damage checkpoint, it is presently unclear how mitotic cells respond to the presence of persistent JMs. Our observations that *sgs1Δ mms4-14A* and *sgs1Δ cdc5-2* double mutants are viable, but are severely impaired in proliferation, therefore provided a tool to study the cellular consequences of impaired JM processing under physiological conditions.

The analysis of *sgs1Δ mms4-14A* and *sgs1Δ cdc5-2* mutants indicated that JMs delay cell cycle progression either at the G2/M transition or after anaphase initiation. To distinguish between these possibilities, we analyzed their ability to undergo anaphase, which is triggered by the proteolytic degradation of the anaphase inhibitor Pds1. Immunofluorescence analysis of Pds1-myc18 showed that a bipolar spindle formed in ~65% of *sgs1Δ mms4-14A* and *sgs1Δ cdc5-2* cells that were positive for nuclear Pds1 staining. In control strains, a lower fraction of cells (32%–45%) with a bipolar spindle was detected (Figure S3A). Because Pds1 accumulates at the G1/S transition and is degraded during anaphase and *sgs1Δ mms4-14A* and *sgs1Δ cdc5-2* mutants accumulate with a G2 DNA content (Figure 4E), our observations of an increase in the fraction of Pds1-positive cells containing a bipolar spindle indicate that cell-cycle progression delay occurs at the G2/M transition.

If *sgs1Δ mms4-14A* and *sgs1Δ cdc5-2* mutants delay anaphase initiation, one expectation is that an abnormal proportion of those cells containing a large bud should be Pds1 positive. This was indeed the case, as immunofluorescence analysis of Pds1 levels showed a striking defect in Pds1 destruction and anaphase initiation (Figure 5A). Indeed, <50% of these mutants entered anaphase, whereas more than 90% of the control strains showed Pds1 destruction and spindle elongation.

We next investigated whether *sgs1Δ mms4-14A* and *sgs1Δ cdc5-2* double mutants accumulate at the G2/M transition due to either DNA replication or DNA damage checkpoint activation. However, we found no evidence for Rad53 phosphorylation, which provides a general readout of checkpoint activation (Figure 5B) (Sanchez et al., 1996; Sun et al., 1996), or for histone H2A phosphorylation, which would be indicative of Mec1/Tel1 activation (Figure S3B) (Downs et al., 2000; Redon et al., 2003).

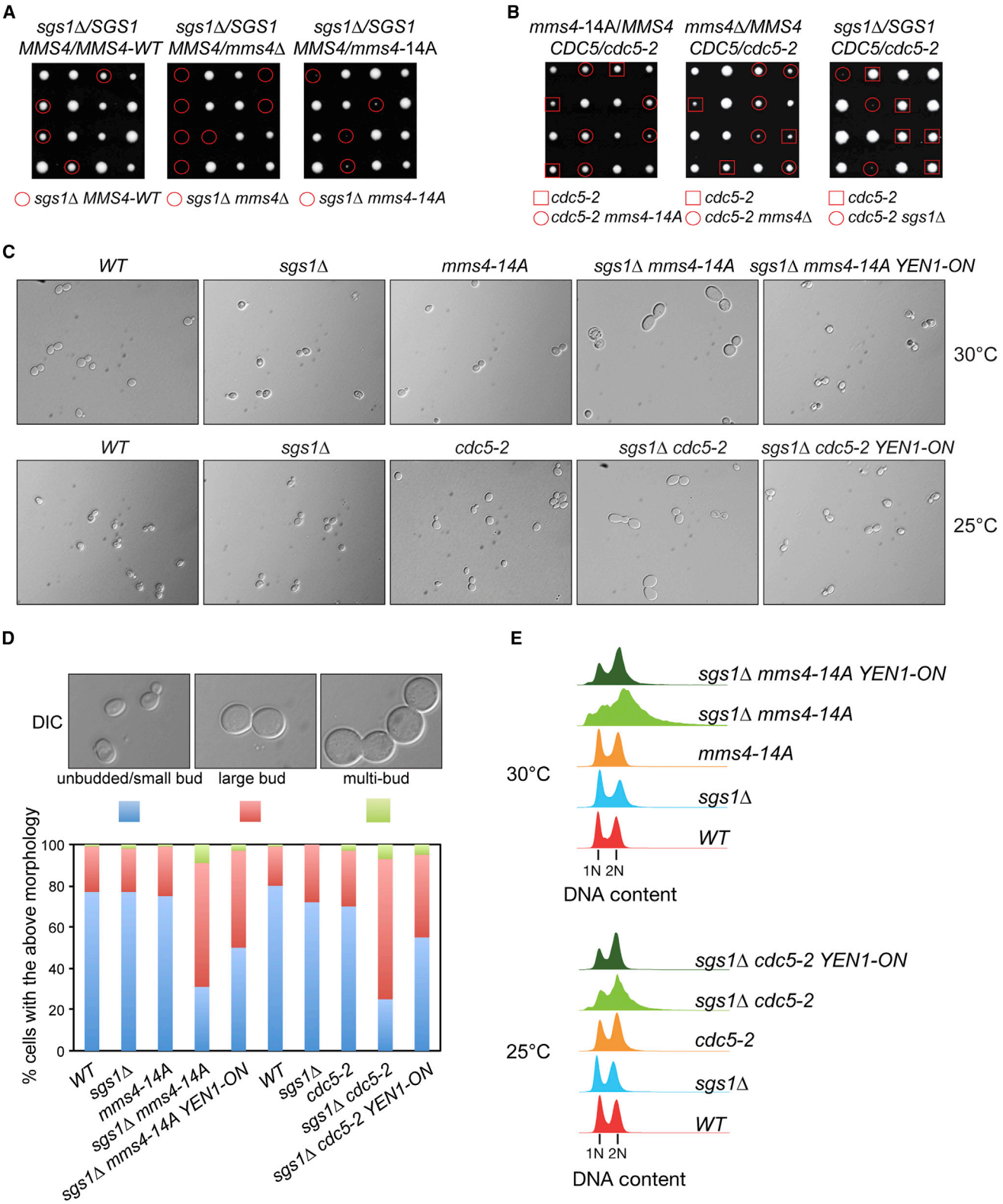

(legend on next page)

These data indicate that in the absence of STR, activation of Mus81-Mms4 at the G2/M transition is required for JM processing, which otherwise trigger a delay in anaphase entry.

Chromosome Segregation Defects and Aneuploidy

To determine whether defective JM processing in *sgs1Δ mms4-14A* and *sgs1Δ cdc5-2* mutants causes additional anaphase defects, we analyzed chromosome segregation in those cells containing a bipolar spindle and lacking Pds1. DAPI staining of DNA from the double mutants showed an abnormally high frequency of anaphase cells containing stretched chromatin or completely unsegregated DNA (Figure 5C). Premature activation of Yen1 (Yen1-ON) substantially rescued this phenotype, consistent with the notion that persistent JMs are the primary cause of chromosome missegregation. Interestingly, in ~10% of all *sgs1Δ mms4-14A* or *sgs1Δ cdc5-2* cells, up to three distinct DNA masses were detectable, irrespective of the cell-cycle stage (Figure 5D). Since these mutants show anaphase defects, the polynucleated cells are likely to originate as a consequence of impaired chromosome segregation, explaining the detection of cells containing >2N DNA (Figure 4E).

These data show that G2/M phosphoactivation of Mus81-Mms4 plays a key role in JM disengagement, in events that are critical for coordinating the completion of DNA repair with chromosome segregation. In the absence of STR, Cdc5-mediated activation of Mus81-Mms4 prevents chromosome missegregation and aneuploidy by ensuring the timely disengagement of JMs.

DISCUSSION

How and why do cells establish such intricate relationships between JM processing enzymes? Important clues to this puzzle originate from evidence for the temporal ordering of JM processing pathways throughout the cell cycle. The Sgs1-Top3-Rmi1 pathway of HJ dissolution operates at early stages and ensures that the primary outcome of recombination is NCO formation. In the absence of STR, or when cells are challenged with DNA damage, JMs are processed later, as cells enter M phase, to generate a mixture of NCOs and COs (Ashton et al., 2011; Dayani et al., 2011). Consistent with this, Mus81-Mms4 and Yen1 activities, which provide the main source of mitotic COs (Ho et al., 2010), are tightly regulated, peaking during metaphase and anaphase, respectively (Matos et al., 2011).

In this work, we provide functional evidence in support of a model whereby the regulated activation of CO-promoting nucleases ensures the timely elimination of JMs that escape STR-mediated dissolution while also minimizing CO formation. Consistent with previous observations, we show that Cdc28/Cdk and Cdc5 promote the phosphorylation and activation of Mus81-Mms4 during M phase (Gallo-Fernández et al., 2012; Matos et al., 2011). In addition, however, we made two important discoveries. First, we found that *cdc5-2* mutants uncouple Mus81-Mms4 phosphoactivation from cell-cycle progression, providing direct evidence that Cdc5 promotes Mus81-Mms4 activation independently of its involvement in cell-cycle progression. Second, we showed that premature Cdc5 expression is sufficient to phosphorylate and activate Mus81-Mms4 independent of the cell cycle stage. These two findings provided unique tools to manipulate the cyclic activation of Mus81-Mms4 and to investigate the consequences of its misregulation.

Polo Kinase Cdc5 Coordinates JM Resolution with Chromosome Segregation

It is well established that polo kinases such as Cdc5 are key regulators of cell-cycle progression and chromosome segregation. In addition, by phosphorylating Mms4, Cdc5 controls the activity of Mus81-Mms4 and defines a very specific window for its function in JM processing. Thus, by simultaneously phosphorylating cohesin (Alexandru et al., 2001), condensin (St-Pierre et al., 2009), and Mus81-Mms4, Cdc5 coordinates the sequential elimination of all types of chromosomal interactions in preparation for efficient chromosome segregation.

Our analysis of *mms4-14A* and *cdc5-2* mutants revealed that late phosphoactivation of Mus81-Mms4 by Cdc5 is critical for DNA repair. Both mutants showed severe sensitivity to DNA damaging agents and failed to efficiently complement *sgs1Δ mms4Δ* double mutants, providing a clear indication of the biological relevance of Mus81-Mms4 regulation during mitosis. Using *sgs1Δ mms4-14A* and *sgs1Δ cdc5-2* double mutants, we also determined the cellular consequences of impaired Mus81-Mms4 activation and deficient JM processing. In the absence of STR, failure to activate Mus81-Mms4 at the G2/M transition caused cell-cycle progression defects such as a delay in anaphase initiation. Although we found no evidence for abnormal levels of DNA damage, as indicated by the lack of DNA damage/replication checkpoint activation, persistent JMs triggered some other checkpoint that monitors the presence of unresolved recombination intermediates. One possibility is that abnormal interchromosomal connections due to unresolved HJs might interfere with the establishment of stable microtubule-kinetochore attachments and that such defects are sensed by the spindle assembly checkpoint and prevent APC/C-mediated anaphase entry (Musacchio and Salmon, 2007).

The importance of mechanisms that delay cell-cycle progression in response to impaired processing of DNA repair intermediates was also highlighted by a second defect in *sgs1Δ mms4-14A* and *sgs1Δ cdc5-2* mutants. Analysis of chromosome segregation revealed that a substantial fraction of anaphase cells displayed asymmetric DNA distribution to the daughter

Figure 4. Hyperactivation of Mus81-Mms4 Is Required for Mitotic Proliferation in the Absence of *SGS1*

(A and B) Diploid strains carrying heterozygous mutations for the indicated wild-type and mutant alleles of *SGS1* and *MMS4* (A) or *CDC5*, *MMS4*, and *SGS1* (B) were microdissected in order to determine synthetic defects in proliferation.

(C) Microscopic inspection (DIC) of exponentially growing liquid cultures of the indicated strains.

(D) Microscopic analysis and quantification of the frequency of the indicated subpopulations in each of the yeast strains visualized in (C). The three images are illustrative and were collected from wild-type and *sgs1Δ mms4-14A* cells.

(E) DNA content analysis by FACS of the yeast cultures imaged in (C).

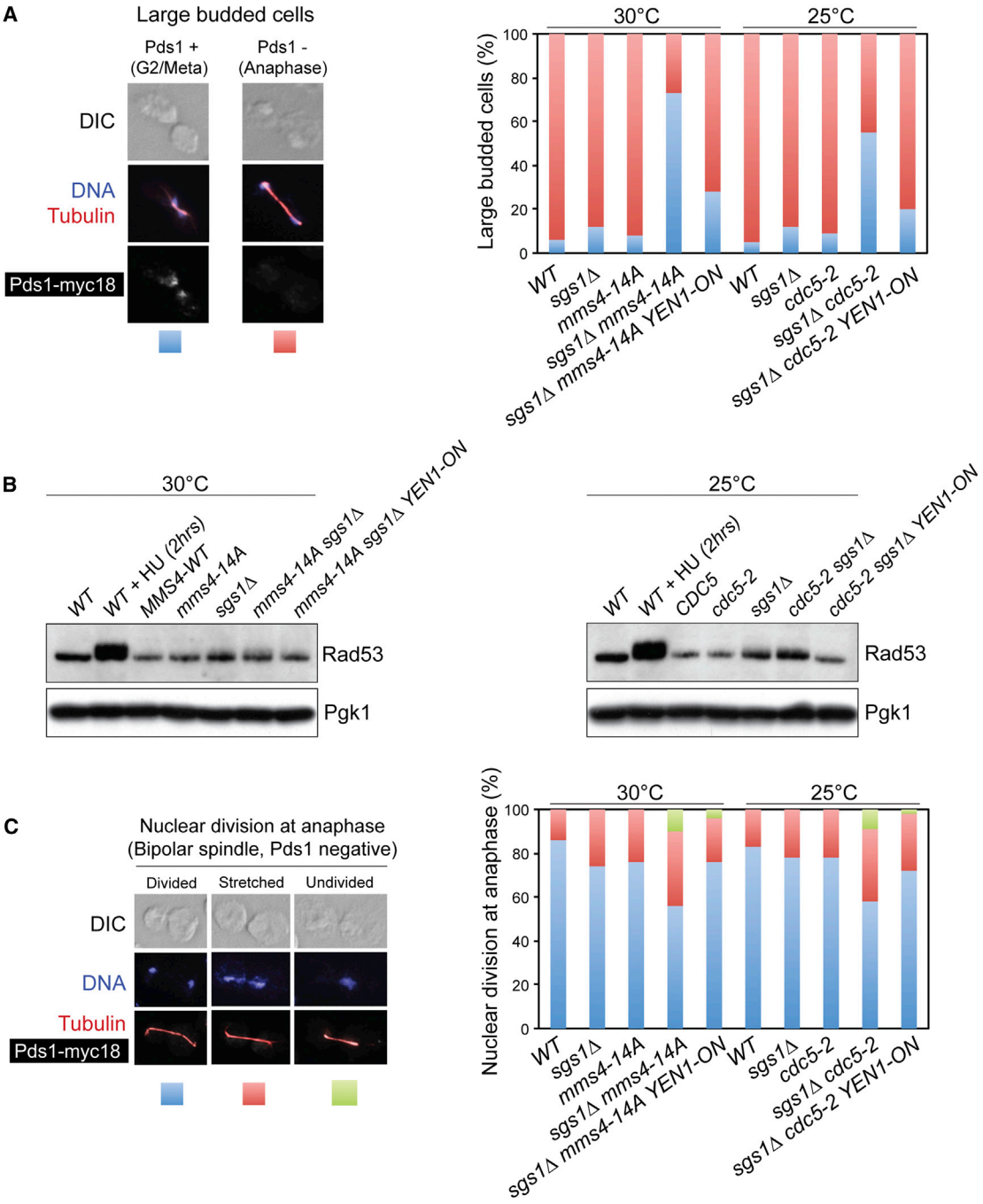

(legend on next page)

cells, consistent with chromosome nondisjunction. This defect was linked to the appearance of multinucleated cells and the detection of aneuploid populations.

Avoiding Mitotic Crossovers while Safeguarding Chromosome Segregation by Ordering the Actions of JM Processing Enzymes

The detrimental consequences of loss of heterozygosity force somatic cells to adopt a number of complementary strategies to prevent reciprocal exchanges between homologous chromosomes (interhomolog COs). During DSB repair, antirecombinases disengage most recombination intermediates at an early stage to generate NCOs. Nonetheless, repair of a fraction of DSBs involves the stable formation of interhomolog JMs containing double HJs (Bzymek et al., 2010), which in meiotic cells are frequently converted to COs (Allers and Lichten, 2001). In mitotically dividing cells, however, STR-mediated dissolution disengages the majority of these JMs to limit CO formation (Dayani et al., 2011; Ira et al., 2003). Here, we show that the temporal restriction of Mus81-Mms4 activation constitutes a mechanism for the prevention of CO formation and reduction of the potential for LOH. By removing the transcriptional control to Cdc5 expression, we engineered cells that prematurely activated Mus81-Mms4, resulting in a significant increase in the occurrence of mitotic COs. Interestingly, a similar increase in the overall frequency of CO was detected in cells lacking STR (Ira et al., 2003) or in cells expressing a phosphomimetic version of Mms4 (Szakal and Branzei, 2013), suggesting that prematurely activated Mus81-Mms4 might directly compete with, and overpower, STR-mediated JM dissolution.

Our data therefore provide functional evidence that STR, Mus81-Mms4, and Yen1 mediate the resolution of recombination intermediates in three temporally distinct and consecutive waves during the mitotic cell cycle. Due to the late activation of Mus81-Mms4 and Yen1 resolvases, STR provides the primary JM processing activity during early stages of the cell cycle and therefore minimizes CO formation. The subsequent activation of the resolvases ensures the disengagement of JMs that might escape STR, safeguarding chromosome segregation and preventing aneuploidy at the cost of increasing the potential for CO formation and LOH. Remarkably, the critical importance of the precise timing of Mus81-Mms4 activation for JM processing is highlighted by the inability of Yen1, which in contrast to Yen1-ON is only activated upon anaphase initiation, to fully compensate for Mus81-Mms4 in JM processing.

Overall, our work suggests that a regulatory network operates to control Mus81-Mms4 function with a threefold purpose: (1) to promote the efficient completion of DNA repair, (2) to prevent the premature processing of DNA repair/replication intermediates and minimize the occurrence of COs, and (3) to ensure JM resolution and thereby safeguard chromosome segregation. Positive interference with the core of this network, by directly modulating the activity of the cell-cycle kinases CDK and PLK1 or by impairing the efficacy of the DNA damage checkpoint (Szakal and Branzei, 2013), might be a strategy used by cancer cells to drive an increase in the frequency of somatic COs and to promote LOH of tumor suppressors.

EXPERIMENTAL PROCEDURES

All experimental procedures are described in detail in Extended Experimental Procedures.

Yeast Strains and Cultures

All strains are detailed in Table S2. Synchronous release of mitotic cultures and DNA damage sensitivity assays were carried out as described (Blanco et al., 2010).

Protein Analysis

Soluble lysates and affinity-purified proteins were analyzed by SDS-PAGE followed by western blotting. For nuclease assays, epitope-tagged proteins were immunoaffinity purified from cellular extracts and washed extensively. The beads were supplemented with 12 μl of resolution buffer (50 mM Tris-HCl [pH 7.5], 3 mM $MgCl_2$) and approximately 1 nM 5′-^{32}P end-labeled synthetic Holliday junction DNA (Ip et al., 2008). After 30–60 min incubation at 30°C, reactions were stopped and radiolabeled products were separated by PAGE and analyzed by autoradiography or phosphorimaging.

Genetic Analysis of Recombination

Analysis of recombination outcome during mitotic DSB repair was performed as described previously (Ho et al., 2010).

SUPPLEMENTAL INFORMATION

Supplemental Information includes Extended Experimental Procedures, three figures, and two tables and can be found with this article online at http://dx.doi.org/10.1016/j.celrep.2013.05.039.

ACKNOWLEDGMENTS

We thank Lorraine Symington for yeast strains, Raphael Chaleil for modeling the Cdc5 structure, and members of our laboratory for comments. This work was supported by Cancer Research UK, the European Research Council, the Louis-Jeantet Foundation, the Swiss Bridge Foundation, and the Breast Cancer Campaign. J.M. was a recipient of a fellowship from the Human Frontiers Science Program.

Received: March 4, 2013
Revised: May 8, 2013
Accepted: May 23, 2013
Published: June 27, 2013

Figure 5. Impaired Joint Molecule Processing Causes a Delay in Anaphase Entry and Chromosome Missegregation

(A) The indicated strains were grown and cells containing a large bud and a bipolar spindle were selected and inspected for the presence (G2/metaphase) or absence of Pds1 (anaphase) by immunofluorescence. Representative images are shown (left) and the quantifications are indicated (right).

(B) Western blot analysis of Rad53 in the indicated strains.

(C) DNA segregation at anaphase (Bipolar spindle, Pds1 negative) was visualized by immunofluorescence (representative images from *sgs1Δ mms4-14A* mutants are shown left) and quantified (right).

(D) Polynucleated cells (i.e., those containing two or more DNA masses), detected in *sgs1Δ mms4-14A* and *sgs1Δ cdc5-2* double mutants, were visualized and quantified. Representative examples of polynucleated cells from *sgs1Δ cdc5-2* cells are shown (right).

See also Figure S3.

REFERENCES

Alexandru, G., Uhlmann, F., Mechtler, K., Poupart, M.A., and Nasmyth, K. (2001). Phosphorylation of the cohesin subunit Scc1 by Polo/Cdc5 kinase regulates sister chromatid separation in yeast. Cell *105*, 459–472.

Allers, T., and Lichten, M. (2001). Differential timing and control of noncrossover and crossover recombination during meiosis. Cell *106*, 47–57.

Ashton, T.M., Mankouri, H.W., Heidenblut, A., McHugh, P.J., and Hickson, I.D. (2011). Pathways for Holliday junction processing during homologous recombination in *Saccharomyces cerevisiae*. Mol. Cell. Biol. *31*, 1921–1933.

Bishop, A.C., Ubersax, J.A., Petsch, D.T., Matheos, D.P., Gray, N.S., Blethrow, J., Shimizu, E., Tsien, J.Z., Schultz, P.G., Rose, M.D., et al. (2000). A chemical switch for inhibitor-sensitive alleles of any protein kinase. Nature *407*, 395–401.

Blanco, M.G., Matos, J., Rass, U., Ip, S.C.Y., and West, S.C. (2010). Functional overlap between the structure-specific nucleases Yen1 and Mus81-Mms4 for DNA-damage repair in *S. cerevisiae*. DNA Repair (Amst.) *9*, 394–402.

Bzymek, M., Thayer, N.H., Oh, S.D., Kleckner, N., and Hunter, N. (2010). Double Holliday junctions are intermediates of DNA break repair. Nature *464*, 937–941.

Dayani, Y., Simchen, G., and Lichten, M. (2011). Meiotic recombination intermediates are resolved with minimal crossover formation during return-to-growth, an analogue of the mitotic cell cycle. PLoS Genet. *7*, e1002083.

Downs, J.A., Lowndes, N.F., and Jackson, S.P. (2000). A role for *Saccharomyces cerevisiae* histone H2A in DNA repair. Nature *408*, 1001–1004.

Fabre, F., Chan, A., Heyer, W.D., and Gangloff, S. (2002). Alternate pathways involving Sgs1/Top3, Mus81/Mms4, and Srs2 prevent formation of toxic recombination intermediates from single-stranded gaps created by DNA replication. Proc. Natl. Acad. Sci. USA *99*, 16887–16892.

Gallo-Fernández, M., Saugar, I., Ortiz-Bazán, M.A., Vázquez, M.V., and Tercero, J.A. (2012). Cell cycle-dependent regulation of the nuclease activity of Mus81-Eme1/Mms4. Nucleic Acids Res. *40*, 8325–8335.

Ho, C.K., Mazón, G., Lam, A.F., and Symington, L.S. (2010). Mus81 and Yen1 promote reciprocal exchange during mitotic recombination to maintain genome integrity in budding yeast. Mol. Cell *40*, 988–1000.

Ip, S.C.Y., Rass, U., Blanco, M.G., Flynn, H.R., Skehel, J.M., and West, S.C. (2008). Identification of Holliday junction resolvases from humans and yeast. Nature *456*, 357–361.

Ira, G., Malkova, A., Liberi, G., Foiani, M., and Haber, J.E. (2003). Srs2 and Sgs1-Top3 suppress crossovers during double-strand break repair in yeast. Cell *115*, 401–411.

Kaliraman, V., Mullen, J.R., Fricke, W.M., Bastin-Shanower, S.A., and Brill, S.J. (2001). Functional overlap between Sgs1-Top3 and the Mms4-Mus81 endonuclease. Genes Dev. *15*, 2730–2740.

Kitada, K., Johnson, A.L., Johnston, L.H., and Sugino, A. (1993). A multicopy suppressor gene of the *Saccharomyces cerevisiae* G1 cell cycle mutant gene *dbf4* encodes a protein kinase and is identified as CDC5. Mol. Cell. Biol. *13*, 4445–4457.

Matos, J., Blanco, M.G., Maslen, S.L., Skehel, J.M., and West, S.C. (2011). Regulatory control of the resolution of DNA recombination intermediates during meiosis and mitosis. Cell *147*, 158–172.

Mullen, J.R., Kaliraman, V., Ibrahim, S.S., and Brill, S.J. (2001). Requirement for three novel protein complexes in the absence of the Sgs1 DNA helicase in *Saccharomyces cerevisiae*. Genetics *157*, 103–118.

Musacchio, A., and Salmon, E.D. (2007). The spindle-assembly checkpoint in space and time. Nat. Rev. Mol. Cell Biol. *8*, 379–393.

Redon, C., Pilch, D.R., Rogakou, E.P., Orr, A.H., Lowndes, N.F., and Bonner, W.M. (2003). Yeast histone 2A serine 129 is essential for the efficient repair of checkpoint-blind DNA damage. EMBO Rep. *4*, 678–684.

Sanchez, Y., Desany, B.A., Jones, W.J., Liu, Q.H., Wang, B., and Elledge, S.J. (1996). Regulation of RAD53 by the ATM-like kinases MEC1 and TEL1 in yeast cell cycle checkpoint pathways. Science *271*, 357–360.

Shirayama, M., Zachariae, W., Ciosk, R., and Nasmyth, K. (1998). The Polo-like kinase Cdc5p and the WD-repeat protein Cdc20p/fizzy are regulators and substrates of the anaphase promoting complex in *Saccharomyces cerevisiae*. EMBO J. *17*, 1336–1349.

St-Pierre, J., Douziech, M., Bazile, F., Pascariu, M., Bonneil, E., Sauvé, V., Ratsima, H., and D'Amours, D. (2009). Polo kinase regulates mitotic chromosome condensation by hyperactivation of condensin DNA supercoiling activity. Mol. Cell *34*, 416–426.

Sun, Z.X., Fay, D.S., Marini, F., Foiani, M., and Stern, D.F. (1996). Spk1/Rad53 is regulated by Mec1-dependent protein phosphorylation in DNA replication and damage checkpoint pathways. Genes Dev. *10*, 395–406.

Szakal, B., and Branzei, D. (2013). Premature Cdk1/Cdc5/Mus81 pathway activation induces aberrant replication and deleterious crossover. EMBO J. *32*, 1155–1167.

Tay, Y.D., and Wu, L. (2010). Overlapping roles for Yen1 and Mus81 in cellular Holliday junction processing. J. Biol. Chem. *285*, 11427–11432.

Wu, L., and Hickson, I.D. (2003). The Bloom's syndrome helicase suppresses crossing over during homologous recombination. Nature *426*, 870–874.

Cell PRESS
Open ACCESS

EXTENDED EXPERIMENTAL PROCEDURES

Yeast Strain Constructions

All strains were derivatives of haploid BY4741, BY4742 or W303, as described in Table S2. The following alleles have been described previously: *cdc28-as1* (Bishop et al., 2000), *cdc5-2 (msd2-1)* (Kitada et al., 1993), *MMS4-myc9, MMS4-WT-ha3*, *mms4-14A-ha3*, *MUS81-myc13* (Matos et al., 2011). *Cdc5-2* and *cdc28-as1* alleles, originally in a W303 background, were backcrossed to BY4742/BY4741.

For galactose-inducible and constitutive expression of eGFP-tagged Cdc5, *CDC5* was cloned into the advanced gateway expression vectors, pAG305GAL-ccdB-EGFP and pAG305GPD-ccdB-EGFP, respectively (Alberti et al., 2007). pGAL-CDC5-EGFP and pGPD-CDC5-EGFP were linearized and integrated at *LEU2*.

The *YEN1-ON* allele encodes for a mutant form of Yen1, which is constitutively active throughout the mitotic cell cycle (M.G.B., J.M., and S.C.W., manuscript in preparation).

To prevent the selection of suppressor mutations that confer a proliferative advantage, yeast strains containing *mms4-14A* or *cdc5-2* in combination with *sgs1Δ* (Figures 4 and 5; and Figure S3) were freshly generated for each experiment. The appropriate haploids carrying single mutations were crossed and the double mutants, or control strains, isolated by tetrad analysis.

Yeast Cultures

For mitotic time courses, BY4741 *MATa* derivatives were grown exponentially in YPD (OD_{600} ~0.3) at 25°C or 30°C and synchronized by addition of α-factor (final concentration 3 μM). After 2–3 hr, the cells (>95% unbudded) were harvested, washed once in YPD and released into one-half volume of YPD. Depending on the experiment and strain, the cultures were incubated at 25°C, 30°C, or 37°C. Cells (50–100 ml) were collected every 15 min, and samples were taken for DNA content analysis and for preparation of protein extracts.

To inhibit Cdc28 or Cdc5 in G2/M enriched cultures, cells were incubated at 25°C for 3.5 hr in the presence of 15 μg/ml nocodazole (Sigma). Cdc28-as1 kinase was inhibited by treating cultures with 5 μM 1NM-PP1 (Santa Cruz) for 30 min. For Cdc5 inhibition, the relevant strains were incubated at 25°C or 37°C for 1 hr.

To induce Cdc5 expression in cells carrying P_{GAL}-*CDC5*, galactose (2%) was added to cultures growing exponentially in $YP_{Raffinose}$ (1% yeast extract, 2% peptone, 2% Raffinose). For G1/S synchronization prior to Cdc5 induction, cultures were pre-treated with 100 mM hydroxyurea for 2.5 hr.

Yeast Protein Analysis

Protein analysis in yeast was performed as described (Matos et al., 2008). Cultures were disrupted using glass beads in 10% TCA. Precipitates were collected by centrifugation, resuspended in 2× sample buffer, and neutralized with 1 M Tris-base. Samples were boiled at 95°C for 10 min, cleared by centrifugation, and separated in NuPAGE 3%–8% Tris-Acetate gels (Invitrogen).

Immunoprecipitates were prepared from 50-100 ml of mitotic cultures. Cells were lysed with glass beads in buffer R (40 mM Tris [pH 7.5], 150 mM NaCl, 10% glycerol, 0.1% NP40) containing protease and phosphatase inhibitors. Protein extracts were cleared and normalized (6-12 mg protein in 500-700 μl) and epitope-tagged proteins were captured using mouse monoclonal antibodies to Myc (9E10), or polyclonal antibodies to HA (Santa Cruz), covalently coupled to agarose beads (AminoLink Plus, Thermo Scientific). For immunoblotting, antibodies to the following proteins or epitope tags were used: HA HRP-conjugated (Rat, 1:1,000, Sigma), HA (mouse monoclonal, 1:1,000, Covance 16B12), Myc HRP-conjugated (Rabbit, 1:5,000, Abcam), Myc (mouse 9E10, 1:1,000, Cancer Research UK), Cdc5 (Goat, 1:200, Santa Cruz), Clb1 (Goat, 1:400, Santa Cruz), Pgk1 (mouse, 1:5,000, Invitrogen), and Rad53 (Goat, 1:1,000, Santa Cruz).

FACS Analysis

Cells were fixed overnight in 70% ethanol at 4°C, washed in 50 mM Tris–HCl (pH 7.8) and resuspended in the same buffer containing 0.1 mg/ml RNase A, and incubated overnight at 37°C. They were then resuspended in 55 mM HCl containing 5 mg/ml pepsin and incubated at 37°C for 20 min. After washing with FACS buffer (180 mM Tris-HCl [pH 7.5], 190 mM NaCl, 70 mM $MgCl_2$), the cells were resuspended in FACS buffer containing 50 μg/ml propidium iodide. Before measurements were taken, the cells were diluted into 1 ml 50 mM Tris-HCl (pH 7.8). Cellular DNA content was determined using a FACScan cytometer (Becton Dickinson) running CellQuest software, and data were processed using FlowJo software.

DNA Damage Sensitivity Assays

Cells grown to mid-log phase were normalized to 0.5×10^7 cells/ml, and 10-fold serial dilutions were spotted onto YPD plates, or YPD plates containing different concentrations of MMS, HU, 4-NQO or CPT. UV sensitivity was assayed by spotting cells on YPD after 10-fold dilution, followed by exposure to UV_{254} light using a CL-1000 UV crosslinker (UVP). Plates were incubated in the dark for 2–4 days, at 25°C, 30°C, or 37°C.

Microscopy Analysis and Quantifications

The quantitative analyses of cell cycle stage-specific parameters (spindle morphology, nuclear division, and Pds1 staining) were performed by the examination of at least 200 cells for each variable.

Fluorescence Microscopy

Yeast cells were processed for immunostaining as described (Salah and Nasmyth, 2000). The primary antibodies were: mouse monoclonal anti-Myc 9E10 (1:100), rat anti-tubulin (1:250, Serotec), rabbit anti-Myc (1:200, Santa Cruz sc-789). Secondary antibodies conjugated to Alexa555 (1:250, Chemicon), Alexa488 (1:200, Chemicon), and Alexa647 (1:100, Chemicon) were used for detection. DNA was stained with 4′,6-diamidino-2-phenylindole (DAPI). Images were acquired using a Zeiss AXIO Imager M1 with a 63x or 100x EC-PLAN-NEOFLUOR lens and Hamamatsu photonics camera under the control of Volocity software. Images were processed using Adobe Photoshop.

Genetic Analysis of DSB-Induced Recombination

Analysis of recombination outcome during mitotic DSB repair was performed as described (Ho et al., 2010; Mazón et al., 2012). In brief, an I-SceI-induced DSB at the *ade2-I* allele is repaired from the homolog, which carries the mutated *ade2-n* allele. The diploid strain carries heterozygous drug-resistance markers distal to *ade2* (*Hph* or *Nat*), and markers on the opposite chromosome arm (*MET22* or *met22::URA3*), which provides a way to detect LOH resulting from recombination-mediated chromosome loss. Red-white-sectored colonies result from G2 repair of one broken chromatid by short-tract gene conversion ($ADE2^+$) and repair of the other broken chromatid by long-tract gene conversion ($ade2^-$). In this class of colonies, which in our experiments represented 20%–40% of all recombinants, a crossover associated with repair of one of the broken chromatids was detected by reciprocal loss of heterozygosity (LOH) of the *Hph* and *Nat* markers, whereas break induced recombination (BIR) results in nonreciprocal LOH.

The experiments were carried out by growing diploids of the relevant genotypes (Table S2) in liquid $YP_{Raffinose}$ medium to an OD_{600} of 0.4. Galactose was added to a final concentration of 2%, to induce I-SceI expression. After 90 min, cells were plated onto YPD medium, incubated for 2 days at room temperature, and replica-plated on YPD, YPD + Hygromycin (Hyg), YPD + Nourseothricin (Nat), SC-Ade, SC-Met, SC-Ura, and SC-Ade+Gal media to discriminate recombination events. Scoring of the type of recombination was performed as described (Mazón et al., 2012). Statistical significance for the differences in the number of CO and NCO events, between all analyzed strains, was estimated through a Chi-square test.

Nuclease Assays

For nuclease assays, immuno-affinity purification was carried out using anti-Myc (clone 9E10) beads. The beads (10 μl) were washed extensively, and then mixed with 12 μl cleavage buffer (50 mM Tris-HCl pH 7.5, 3 mM $MgCl_2$) and 5′-^{32}P-end-labeled synthetic Holliday junction X26 DNA (~1 nM) (Ip et al., 2008). After 45-60 min incubation with gentle rotation, at 30°C or 37°C, reactions were stopped by addition of 2.5 μl of 10 mg/ml proteinase K and 2% SDS. Loading buffer was added and radiolabeled products were separated by 10% PAGE, and analyzed by autoradiography or by phosphorimaging using a Typhoon scanner and ImageQuant software. Resolution activity was calculated by determining the fraction of nicked duplex DNA product relative to the sum of the intact substrate and resolution product.

SUPPLEMENTAL REFERENCES

Alberti, S., Gitler, A.D., and Lindquist, S. (2007). A suite of Gateway cloning vectors for high-throughput genetic analysis in *Saccharomyces cerevisiae*. Yeast *24*, 913–919.

Matos, J., Lipp, J.J., Bogdanova, A., Guillot, S., Okaz, E., Junqueira, M., Shevchenko, A., and Zachariae, W.G. (2008). Dbf4-dependent CDC7 kinase links DNA replication to the segregation of homologous chromosomes in meiosis I. Cell *135*, 662–678.

Mazón, G., Lam, A.F., Ho, C.K., Kupiec, M., and Symington, L.S. (2012). The Rad1-Rad10 nuclease promotes chromosome translocations between dispersed repeats. Nat. Struct. Mol. Biol. *19*, 964–971.

Salah, S.M., and Nasmyth, K. (2000). Destruction of the securin Pds1p occurs at the onset of anaphase during both meiotic divisions in yeast. Chromosoma *109*, 27–34.

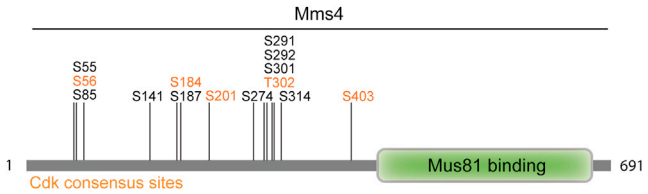

Figure S1. Identified and Mutated Phosphorylation Sites in Mms4, Related to Figure 1

Diagram of Mms4, indicating the 14 phosphorylation sites mutated to alanine in Mms4-14A. Cdk consensus sites are highlighted.

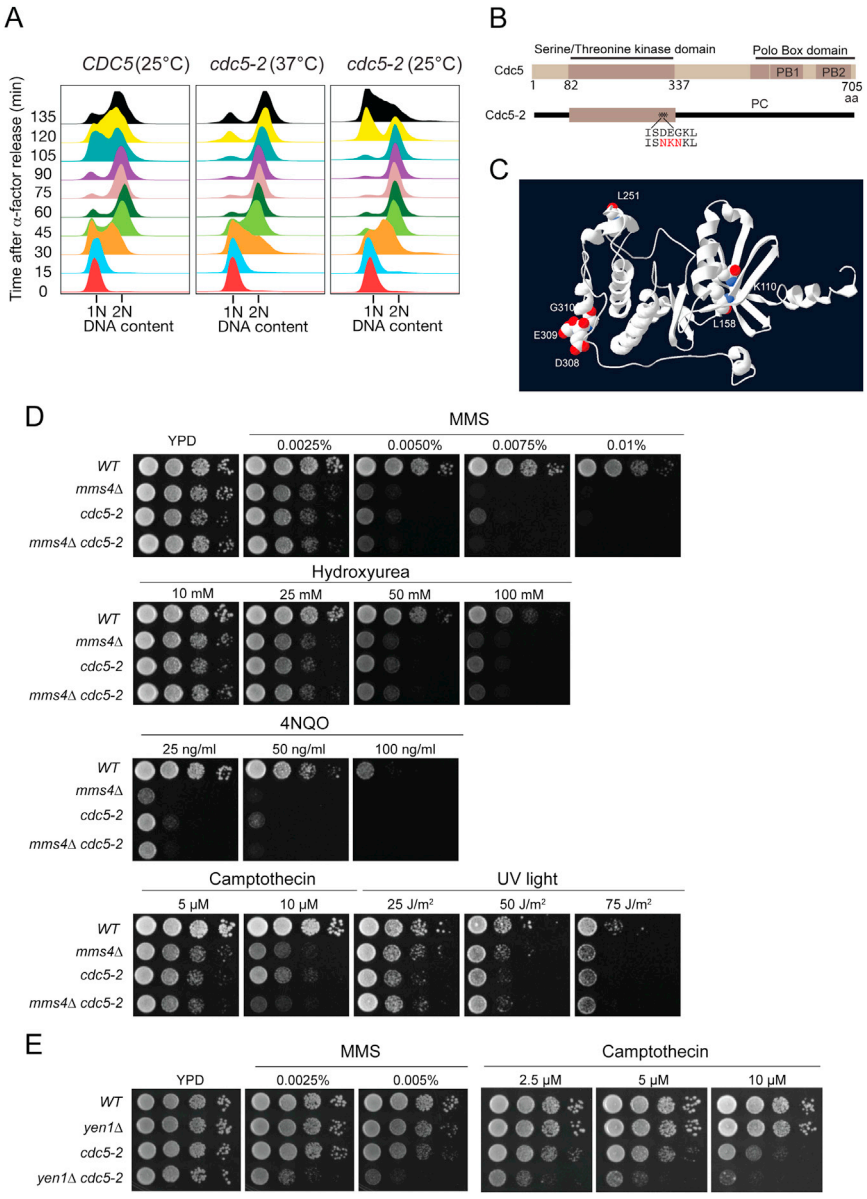

Figure S2. Analysis of the Role of Cdc5 in Mus81-Mms4 Hyperactivation and DNA Repair, Related to Figure 2

(A) Cellular DNA content of *CDC5* or *cdc5-2* strains expressing *MMS4-myc9*, synchronized with α-factor and released to undergo mitosis, was measured by FACS analysis. The cells were grown at the indicated temperatures.

(B) Graphic illustration of the Cdc5 mutations (D308N, E309K and G310N) present in *cdc5-2* strains.

(C) Modeling of the kinase domain of *Saccharomyces cerevisiae* Cdc5 showing the position of the residues mutated in Cdc5-2 and, for comparison, the mutated residues in cdc5-ad (L251), kinase dead Cdc5 (K110), and cdc5-as1 (L158).

(D) Expanded version of Figure 2B. Serial ten-fold dilutions of the indicated strains grown to mid-log phase were normalized, and spotted in YPD plates containing the indicated amounts of DNA damaging agents. Cells were grown for 3 days at 25°C.

(E) Expanded version of Figure 2D.

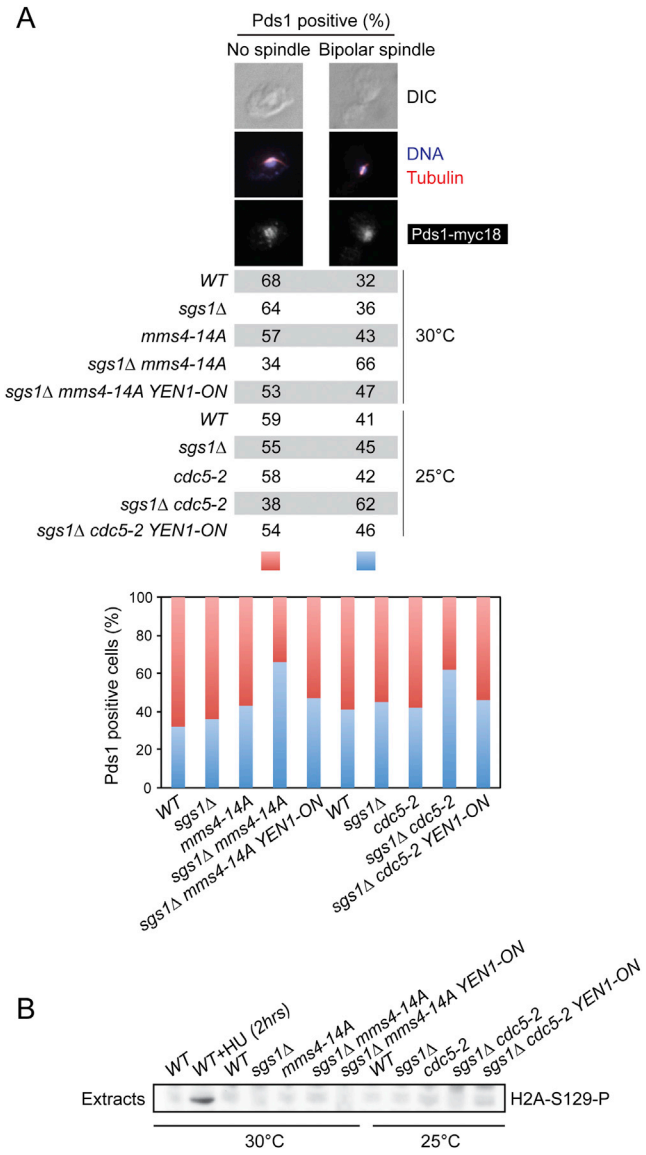

Figure S3. Mutants with Impaired JM Processing Accumulate at the G2/M Transition, Related to Figure 5

(A) Immunofluorescence analysis of the frequency of G2/metaphase cells in cultures of the indicated genotypes. Pds1-positive cells were analyzed for the absence (S-phase/G2) or presence of a bipolar spindle (G2/metaphase).

(B) Western-blot analysis for histone H2A phosphorylation at S129 in the indicated strains.